International Journal of Current Research and Review
DOI: http://dx.doi.org/10.31782/IJCRR.2022.14902

Research Article

IJCRR
Section: Healthcare
ISI Impact Factor (2021-22): 2.176
IC Value (2020): 91.47
SJIF (2020) = 7.893

Predicted Interactionsof Cyclooxygenase2 with Nasopharyngeal Cancer-linked Ribosomal Proteins, uS19 and eL27

Alyaa Syafiqah Binti Shamsuri[1], Edmund Ui-Hang Sim[1*]

[1]Faculty of Resource Science and Technology, UniversityMalaysia Sarawak, 94300 Kota Samarahan, Sarawak, Malaysia.

ABSTRACT

Introduction: The Cyclooxygenase 2 (COX-2) and ribosomal proteins (RP) of uS19 and eL27 were reported to be associated with nasopharyngeal cancer (NPC). However, there is no studies on their interactions.

Objective/Aim: This study aimed to extrapolated the interactions of COX-2 with uS19 and eL27 via *in silico* approach.

Methods: Bioinformatics analysis involving the web-based applications of SWISS-MODEL, ClusPro, FireDock/PatchDock and Protein Interaction Calculator (PIC), and the UniProfKB database were used for the purpose of our study.

Results: We revealed possible interactions between uS19 and eL27 with COX-2 individually. Evaluation of the interacting interface amino acid residues of the uS19-COX2 and eL27-COX2 complexes show hydrophobic and ionic bonds in the former and only hydrophobic bonds in the latter.

Conclusion: Our findings provide novel *in silico* evidence of COX-2's interactions with two NPC-associated RPs (uS19 and eL27), and propose an interplay among these proteins during the oncogenesis of NPC.

Key Words: Cyclooxygenase 2, Nasopharyngeal carcinoma, Molecular docking, Protein-protein interaction, Ribosomal proteins, uS19 (S15), eL27 (L27)

INTRODUCTION

Cyclooxygenase (COX) has two isoforms which are Cyclooxygenase-1 (COX-1) and Cyclooxygenase-2 (COX-2). While COX-1 is commonly present in normal tissues and responsible for physiological processes, COX-2 is associated with physiological stress and diseases such as inflammation and cancers respectively.[1] COX-2 represses tumour immunity and promote tumour growth[2] suggesting an association of its over-expression with carcinogenesis. In fact, COX-2 overexpression has been found in nasopharyngeal cancer (NPC)[3] with significant poor prognosis in overall survival rate among patients[4]. Hence, identifying oncogenic factors that it interacts with will be essential in unravelling the molecular events mediated by COX-2 during NPC oncogenesis.

The roles of ribosomal proteins (RPs) in tumourigenesis are widely known[5,6,7] including during the carcinogenesis of human nasopharyngeal carcinoma (NPC).[8] Two RPs that are associated with NPC are eL27 and uS19 – both reportedly upregulated in NPC.[9,10,11] However, to date, there is limited information on the molecular pathways and network (particularly, the interacting partners) of these RPs during NPC oncogenesis. More precisely, the relationships of COX-2 with eL27 and uS19 have never been studied before this.

Interactions among proteins are essential biological processes for normal cellular physiology, but when these interactions are perturbed or dysregulated, they can lead to diseases, including cancer. Post-translational modifications and protein-protein interactions (PPI) involving COX-2 have been explained.[12] Nevertheless, the association of COX-2 specifically with eL27 and/or uS19 has never been investigated. Likewise, the link between eL27 with various factors of NPC pathogenesis have been suggested[11] but never yet with COX-2. Similarly, despite uS19's suspected relationship with Epstein-Barr Virus (EBV) – encoded proteins (EBV is an established viral agent linked to causation of NPC),[13]

Corresponding Author:
Professor Dr. Edmund Ui-Hang Sim, Faculty of Resource Science and Technology, University Malaysia Sarawak, 94300 Kota Samarahan, Sarawak, Malaysia; Fax: +60-82-583160; E-mail: uhsim@unimas.my

ISSN: 2231-2196 (Print) **ISSN:** 0975-5241 (Online)

Received: 10.03.2022 **Revised:** 02.04.2022 **Accepted:** 19.04.2022 **Published:** 03.05.2022

its association with COX-2 remains unresolved. Therefore, studies to investigate the possibilities of PPI of COX-2 with eL27 and uS19 are warranted.

There is increasing relevance of employing computational methods and bioinformatics resources to analyse PPI. This is especially so when experimental approaches are time-consuming, labour-intensive, and costly. Moreover, experimental methods are not applicable to all types of protein,[14] have limited usefulness in identifying weak and transient interactions,[15] and are prone to false positive/negative outcomes.[16,17,18] Advancement in computational methods for PPI[19] coupled with the growth of protein big data has made in silico analysis an essential approach to complement experimental methods in identifying protein interaction. Taking on this approach, we herein present findings on the computationally predicted interaction between the COX-2 protein with two NPC associated RPs, uS19 and eL27.

METHODS

Acquisition of three-dimensional (3D) protein structures

The 3D structures of uS19, eL27 and COX-2 proteins were needed to perform the computational prediction. UniProt Knowledgebase (UniProtKB) database was used to search for the protein structures. Each protein was searched using its name under the '*Homo sapiens*' category. Only the structure of COX-2 was available from UniProt KB and suitable to be used for further analysis. The PDB file of the structure was downloaded. Individual structure of both ribosomal proteins uS19 and eL27 were not available from UniProt KB.

Construction of the 3D structural model of ribosomal proteins

The 3D models of uS19 and eL27 proteins were built using SWISS-MODEL Workspace. Construction was done via the publicly accessible server.[20] The principle is based on homology modelling where existing homologous protein structures that served as templates were used to predict and generate the 3D model of the target proteins.[21,22] In this study, the FASTA-formatted files of the amino acid sequences of uS19 and eL27 were firstly obtained from National Centre for Biotechnology Information (NCBI) and is used as the input for the SWISS-MODEL Workspace website. For the uS19, two isoforms are available in NCBI, and Isoform 2 was chosen as it has 100% sequence identity to the template. Isoform 1 has 99.31% sequence identity. The PDB file of the constructed uS19 and eL27 models was used for further analysis.

Evaluation of 3D structural models of ribosomal proteins

Quality assessment for the protein models is necessary to reduce structurally inaccurate data prior to further analysis.[23,24] QMEAN score, Ramachandran plot, RMSD value, ERRAT and VERIFY 3D score of the models were taken as qualifying parameters. The QMEAN score of each model was obtained from the SWISS-MODEL server. A good QMEAN score is one that does not deviate more than 1 standard deviation from the mean score of those proteins that are similar in size and with high-resolution X-ray structures and scores.[24] In other words, a score of around zero indicates a high-quality model. Ramachandran plot of the models was also obtained to check for their stereochemical quality through structure assessment from SWISS-MODEL. Models with higher percentage of Ramachandran-favoured region indicates a high-quality model structure. ERRAT error analysis was for assessment of the non-covalent interactions of various atoms in the structure by comparing with a high-quality structure.[25] VERIFY 3D assays were employed to assess the compatibility of the models with their own amino acid sequence.[26,27] Root-mean-square deviation (RMSD) value for each model was generated using PyMOL2. The RMSD value measures the distance between similar atoms of two protein structures to determine similarity between them upon superimposition.

Molecular docking

Molecular docking of the proteins was done via ClusPro server.[28,29,30] The three steps involved, 1) rigid body docking using PIPER that utilizes the scoring function as well as a pairwise potential; 2) The clustering of the 1000 lowest energy structures based on RMSD to search for the largest clusters with the most probable models of the docked complex; and 3) evaluation and refinement of the selected structures based on energy minimization. The pairing for the docking was done as follow: uS19 with COX-2 and eL27 with COX-2 whereby uS19 and eL27 are the receptors and COX-2, the ligand. Only one solution was chosen to represent the docked complex from the balanced category that has the highest cluster size and lowest free energy. The interface residues contact of the docked complex were obtained using Swiss PdbViewer software version 4.1 (with option less than 5 Å were chosen). Residues were considered to be in close contact if the distance between two closest atoms was ≤ 6 Å.[31]

Evaluation and refinement of the docked complexes

Quality evaluation of the docked complexes were done via dual docking analysis using PatchDock paired with FireDock. PatchDock is based on a geometry-based molecular docking algorithm that assesses docked complexes with respect to an acceptable molecular shape complementarity.[32] The PatchDock results were refined through FireDock programme[33]

whereby optimization that resolves the flexibility problems in the side-chains[34] and refinements of the relative molecular orientation[33] were done. The pairing of uS19 with COX-2 and eL27 with COX-2 were evaluated. Only the best solutions were chosen to be used for dual docking analysis with the complexes from ClusPro. PyMOL2-generated RMSD values of the complexes were used to quantify the assessment.

Evaluation of the interactions of the docked complexes

The docked complexes were examined to identify the types of interactions occurred. This was done using Protein Interactions Calculator (PIC) which calculated the various interactions from the tertiary structure of the docked complex based on standard criteria.[35] Hydrophobic interaction that contributes in the stability of the interaction[36] and ionic interactions of the residues were assessed. The PDB files of the complexes from ClusPro analysis were used for this purpose. Interactions resolution option of less than 5 Å were selected for evaluation.

RESULTS

3D model structures of ribosomal proteins

The 3D structural models of uS19 and eL27 (Figure 1 a & b) was generated using SWISS-MODEL Workspace server and structural assessment value of QMEAN scores and Ramachandran plots are shown in Table 1. Quality evaluation (Table 1) of the models based on ERRAT and VERIFY3D and the RMSD values as obtained via PyMOL indicated validity of these computational models for use in further analysis

Molecular docking and assessment of docked complexes

uS19 – COX-2 complex

The complex generated from ClusPro [Fig. 2 (a)] was obtained from the balanced category with the highest cluster size: 123 and lowest free energy (-1031.0 kcal/mol). On the other hand, the best solution from PatchDock/FireDock is the complex [Fig. 2(b)] with the lowest global free energy (0.66 kcal/mol). Upon dual docking analysis, the RMSD value obtained via PyMOL2 analysis is 1.557Å. A score of less than 2.0 Å indicates high similarity between the two docked complexes and ascertains the consistency of the docking simulation. Thus, the uS19-COX-2 complex model is deemed as valid prediction and amenable for further analysis on interacting interface residues.

Interface residues of the docked complex with option less than 5Å (based on Swiss PdbViewer) are illustrated in Fig. 2(c) and listed in Table 2. The PIC evaluation of the hydrophobic and ionic interactions of residues under 5 Å is listed in Table 3, which showed the presence of amino acid residues involved in hydrophobic and ionic interactions within the complex. Hydrophobic interactions are important consideration in assessing binding affinity of docked complexes because they contribute to the stabilization of the complex[36]. Hence, our results here provide novel *in silico* evidence of plausible interactions between the two proteins.

eL27 – *COX-2 complex*

From ClusPro analysis [Fig. 3 (a)] the complex generated was obtained from the balanced category with the highest cluster size: 94 and lowest free energy (-1037.5 kcal/mol). However, the best solution obtained from PatchDock/FireDock was the docked complex with lowest global free energy, -26.38 kcal/mol [Fig. 3 (b)]. Dual docking analysis via PyMOL2 revealed a RMSD value of 1.527 Å. The low value (< 2.0 Å) means high similarity between the two docked complex models and consistency in the docking simulation outcomes. Therefore, the eL27-COX-2 complexes [Fig. 3(a) and (b)] are considered reliable predictions amenable for discernment of interface amino acid residues at the vicinities of interaction [Fig. 3(c)]. Interface residues of the docked complex with option less than 5Å (based on Swiss PdbViewer) are shown in Fig. 3(c) and listed in Table 4. The PIC evaluation of the hydrophobic and ionic interactions of residues under 5 Å is listed in Table 5. Our results revealed possible residues involved in hydrophobic and ionic interaction within the complex. The presence of predicted hydrophobic interactions shows that the computationally simulated interaction between eL27 and COX-2 is acceptable.

DISCUSSION

The results of this study show that both RPs (uS19 and eL27) potentially interact with COX-2 protein as demonstrated in molecular docking simulations. In the context of uS19 and COX-2, both have been linked to NPC oncogenesis. COX-2 is highly expressed in NPC[3,37] and is involved in the angiogenesis, tissue invasion and apoptotic resistance.[2] It is also the most potent prognosis marker for NPC.[4] The expression of uS19 genes was also found to be upregulated in NPC[10]. Based on the fact that uS19 and COX-2 are associated with NPC, their predicted interaction has physiological relevance rather than just a computational scenario. Moreover, the relationship of COX-2 with Epstein-Barr virus (EBV) (an established causative factor of NPC) as observed in the induction of COX-2 expression by an EBV-encoded oncoprotein, the latent membrane protein 1 (LMP1) has been reported.[38] There is also *in silico* evidence of extrapolated interaction between uS19 and LMP1.[13] Circumstantially, this suggests the induction of COX-2 by LMP1 via the intermediary role of uS19 – a novel hypothesis that explains the elevated ex-

pression of COX-2 in EBV-positive NPC. Nonetheless, more experimental studies are warranted to test this hypothesis.

In the case of eL27, over-expression has been observed at both transcript and protein levels in NPC cells.[9,11] Two of the pathophysiological progressions of NPC that are putatively mediated by eL27 include tissue invasion and anti-apoptosis.[11] Incidentally, amongst the pathogenesis mechanisms that COX-2 plays in NPC tumorigenesis are tissue invasion and inhibition of apoptosis.[2] Therefore, it is not an untenable notion to suspect an interaction between eL27 and COX-2 in the oncogenesis of NPC. Our data is the first to provide a hypothetical protein-protein interaction model between eL27 and COX-2 albeit limited to computationally-derived results. Experimental proof of the eL27-COX-2 complex and mechanism(s) of its action in the context of NPC tumorigenesis will require further research.

CONCLUSION

Based on a bioinformatics approach that includes homology modelling, model quality assessment, and molecular docking simulation, we have provided *in silico* evidences of direct protein-protein interaction between COX-2 and each of the ribosomal proteins, uS19 and eL27. Since these factors are also associated with NPC oncogenesis, our findings provide novel conceptual insights into the molecular pathway(s)/mechanism(s) mediated by these three proteins in the pathological development of the human nasopharynx.

ACKNOWLEDGEMENT

The authors acknowledge the support of University Malaysia Sarawak in the research work and the reporting of findings that pertain to this study.

Source of funding:

Not applicable.

Conflict of Interest:

The authors declare no conflict of interest.

Authors' Contribution:

Alyaa Syafiqah Binti Shamsuri performed the data analysis, interpreted the results, and wrote the manuscript. Edmund Ui-Hang Sim designed the study, interpreted the results, and co-wrote the manuscript. All authors have read and approved of the final version of the manuscript.

REFERENCES

1. Dubois RN, Abramson SB, Crofford L, Gupta RA, Simon LS, Van De Putte LB, et al. Cyclooxygenase in biology and disease. FASEB J 1998 Sep;12(12):1063-73.
2. Liu B, Qu L, Yan S. Cyclooxygenase-2 promotes tumor growth and suppresses tumor immunity. Cancer Cell Int 2015 Nov 5;15:106. doi: 10.1186/s12935-015-0260-7.
3. Pan J, Tang T, Xu L, Lu JJ, Lin S, Qiu S, et al. Prognostic significance of expression of cyclooxygenase-2, vascular endothelial growth factor, and epidermal growth factor receptor in nasopharyngeal carcinoma. Head Neck 2013 Sep;35(9):1238-47.
4. Sim CC, Sim EU. Over-expression of cyclo-oxygenase-2 predicts poor survival of patients with nasopharyngeal carcinoma: a meta-analysis. J LaryngolOtol 2020 Apr;134(4):338-43.
5. de Las Heras-Rubio A, Perucho L, Paciucci R, Vilardell J, LLeonart ME. Ribosomal proteins as novel players in tumorigenesis. Cancer Metastasis Rev 2014 Mar;33(1):115-41.
6. Zhou X, Liao WJ, Liao JM, Liao P, Lu H. Ribosomal proteins: functions beyond the ribosome. J Mol Cell Biol 2015 Apr;7(2):92-104.
7. Xu X, Xiong X, Sun Y. The role of ribosomal proteins in the regulation of cell proliferation, tumorigenesis, and genomic integrity. Sci China Life Sci 2016 Jul;59(7):656-72.
8. Sim EU, Lee CW, Narayanan K. The roles of ribosomal proteins in nasopharyngeal cancer: culprits, sentinels or both. Biomark Res 2021 Jun 30;9(1):51. doi: 10.1186/s40364-021-00311-x.
9. Sim EU, Chan SL, Ng KL, Lee CW, Narayanan K. Human Ribosomal Proteins RPeL27, RPeL43, and RPeL41 Are Upregulated in Nasopharyngeal Carcinoma Cell Lines. Dis Markers 2016;2016:5179594. doi: 10.1155/2016/5179594.
10. Sim EU, Chee CS, Vasudevan LI, Ng KL, Chan SL. Selective differential expression of the ribosomal protein genes eL14 and uS19 in a well-differentiated epithelial cell line of nasopharyngeal carcinoma. Malays ApplBiol 2018;47(1):247-53.
11. Sim EU, Yew KL. Putative target proteins of the ribosomal protein, RPEL27 in nasopharyngeal carcinoma cells. Malay J Biochem Mol Biol 2019;22(3):48-54.
12. Alexanian A, Sorokin A. Cyclooxygenase 2: Protein-protein interactions and posttranslational modifications. Physiol Genomics 2017 Nov 1;49(11):667-81.
13. Sim EU, Talwar SP. *In silico* evidence of de novo interactions between ribosomal and Epstein - Barr virus proteins. BMC Mol Cell Biol. 2019 Aug 15;20(1):34.
14. Rao VS, Srinivas K, Sujini GN, Kumar GN. Protein-protein interaction detection: methods and analysis. Int J Proteomics 2014;2014:147648. doi: 10.1155/2014/147648.
15. NgounouWetie AG, Sokolowska I, Woods AG, Roy U, Loo JA, Darie CC. Investigation of stable and transient protein-protein interactions: Past, present, and future. Proteomics 2013 Feb;13(3-4):538-57.
16. Serebriiskii IG, Golemis EA. Two-hybrid system and false positives. InTwo-Hybrid Systems 2001 (pp. 123-134). Humana Press.
17. Gingras AC, Gstaiger M, Raught B, Aebersold R. Analysis of protein complexes using mass spectrometry. Nat Rev Mol Cell Biol. 2007 Aug;8(8):645-54.
18. Huang H, Bader JS. Precision and recall estimates for two-hybrid screens. Bioinformatics. 2009 Feb 1;25(3):372-8.
19. Ding Z, Kihara D. Computational Methods for Predicting Protein-Protein Interactions Using Various Protein Features. CurrProtoc Protein Sci 2018 Aug;93(1): e62. doi: 10.1002/cpps.62.
20. Guex N, Peitsch MC, Schwede T. Automated comparative protein structure modelling with SWISS-MODEL and Swiss-PdbViewer: a historical perspective. Electrophoresis 2009 Jun;30 Suppl1:S162-73.
21. Bienert S, Waterhouse A, de Beer TA, Tauriello G, Studer G, Bordoli L, et al. The SWISS-MODEL Repository-new features

and functionality. Nucleic Acids Res 2017 Jan 4;45(D1):D313-D319. doi: 10.1093/nar/gkw1132.
22. Waterhouse A, Bertoni M, Bienert S, Studer G, Tauriello G, Gumienny R, et al. SWISS-MODEL: homology modelling of protein structures and complexes. Nucleic Acids Res 2018 Jul 2;46(W1):W296-W303. doi: 10.1093/nar/gky427.
23. Benkert P, Künzli M, Schwede T. QMEAN server for protein model quality estimation. Nucleic Acids Res 2009 Jul;37(Web Server issue):W510-4. doi: 10.1093/nar/gkp322.
24. Benkert P, Biasini M, Schwede T. Toward the estimation of the absolute quality of individual protein structure models. Bioinformatics 2011 Feb 1;27(3):343-50.
25. Colovos C, Yeates TO. Verification of protein structures: patterns of nonbonded atomic interactions. Protein Sci 1993 Sep;2(9):1511-9.
26. Bowie JU, Lüthy R, Eisenberg D. A method to identify protein sequences that fold into a known three-dimensional structure. Science 1991 Jul 12;253(5016):164-70.
27. Lüthy R, Bowie JU, Eisenberg D. Assessment of protein models with three-dimensional profiles. Nature 1992 Mar 5;356(6364):83-5.
28. Kozakov D, Beglov D, Bohnuud T, Mottarella SE, Xia B, Hall DR, et al. How good is automated protein docking? Proteins 2013 Dec;81(12):2159-66.
29. Kozakov D, Hall DR, Xia B, Porter KA, Padhorny D, Yueh C, et al. The ClusPro web server for protein-protein docking. Nat Protoc 2017 Feb;12(2):255-78.
30. Vajda S, Yueh C, Beglov D, Bohnuud T, Mottarella SE, Xia B, et al. New additions to the ClusPro server motivated by CAPRI. Proteins 2017 Mar;85(3):435-44.
31. Ofran Y, Rost B. Analysing six types of protein-protein interfaces. J Mol Biol 2003 Jan 10;325(2):377-87.
32. Schneidman-Duhovny D, Inbar Y, Nussinov R, Wolfson HJ. PatchDock and SymmDock: servers for rigid and symmetric docking. Nucleic Acids Res 2005 Jul 1;33(Web Server issue):W363-7. doi: 10.1093/nar/gki481.
33. Andrusier N, Nussinov R, Wolfson HJ. FireDock: fast interaction refinement in molecular docking. Proteins 2007 Oct 1;69(1):139-59.
34. Mashiach E, Schneidman-Duhovny D, Andrusier N, Nussinov R, Wolfson HJ. FireDock: a web server for fast interaction refinement in molecular docking. Nucleic Acids Res 2008 Jul 1;36(Web Server issue): W229-32. doi: 10.1093/nar/gkn186.
35. Tina KG, Bhadra R, Srinivasan N. PIC: Protein Interactions Calculator. Nucleic Acids Res2007 Jul;35(Web Server issue):W473-6. doi: 10.1093/nar/gkm423.
36. Chothia C, Janin J. Principles of protein-protein recognition. Nature 1975 Aug 28;256(5520):705-8.
37. Tan KB, Putti TC. Cyclooxygenase 2 expression in nasopharyngeal carcinoma: immunohistochemical findings and potential implications. J Clin Pathol. 2005 May;58(5):535-8.
38. Murono S, Inoue H, Tanabe T, Joab I, Yoshizaki T, Furukawa M, et al. Induction of cyclooxygenase-2 by Epstein-Barr virus latent membrane protein 1 is involved in vascular endothelial growth factor production in nasopharyngeal carcinoma cells. Proc Natl Acad Sci U S A 2001 Jun 5;98(12):6905-10.

Table 1: Quality assessment of 3D model structures uS19 and eL27

	uS19	eL27
Ramachandran Plot		
Residues in favoured region (%)	92.2	87.5
Residues in allowed region (%)	7.8	11.7
Residues in outlier region (%)	0.0	0.8
QMEAN	-0.71	-0.48
RMSD (Å)	0.145	0.152
ERRAT	96.1165	92.6829
VERIFY3D (%)	64.17	95.56

Table 2: Interface residues of the uS19-COX-2 complex

Protein	Interface Residues (<5 Å)
uS19	PHE15 THR16 ARG18 GLY19 VAL20 ASP21 LEU22 ASP23 GLN24 LEU26 ASP27 MET28 GLN32 LYS64 LYS65 ALA67 PRO68 PRO69 MET70 GLU71 LYS72 PRO73 PRO87 VAL90 GLY91 GLU106 PRO109
COX-2	TYR65 THR71 PRO72 GLU73 PHE74 ARG77 ILE78 LYS79 PHE81 LEU82 LYS83 PRO84 THR85 THR88 VAL89 ILE92 LEU93 PHE99 TRP100 PHE107 LEU108 ALA111 ILE112 SER114 TYR115

Table 3: PIC evaluation of the interactions of uS19-COX-2 complex

Interaction	Position	Residue	Chain	Position	Residue	Chain
Hydrophobic	20	VAL	uS19	108	LEU	COX-2
	22	LEU	uS19	82	LEU	COX-2
	26	LEU	uS19	82	LEU	COX-2
	28	MET	uS19	107	PHE	COX-2
	67	ALA	uS19	74	PHE	COX-2
	69	PRO	uS19	65	TYR	COX-2
	69	PRO	uS19	74	PHE	COX-2
	70	MET	uS19	72	PRO	COX-2
	73	PRO	uS19	81	PHE	COX-2
	90	VAL	uS19	81	PHE	COX-2
	90	VAL	uS19	82	LEU	COX-2
	109	PRO	uS19	82	LEU	COX-2
Ionic	23	ASP	uS19	79	LYS	COX-2
	27	ASP	uS19	79	LYS	COX-2
	71	GLU	uS19	77	ARG	COX-2

Table 4: Interface residues of the eL27-COX-2 complex

Protein	Interface Residues (<5 Å)
eL27	GLY2 LYS3 PHE4 LEU12 LEU14 ALA15 GLY16 ARG17 LYS73 TYR75 ASN78 HIS79 MET81 PRO82 THR83 ARG84 TYR85 TRP129 LEU134 ARG135 PHE136
COX-2	PHE81 LEU82 LYS83 PRO84 THR85 THR88 VAL89 TYR91 ILE92 LEU93 PHE96 GLY98 PHE99 TRP100 VAL102 PHE107 LEU108 ALA111 ILE112 TYR115

Table 5: PIC evaluation of the interactions of eL27-COX-2 complex

Interaction	Position	Residue	Chain	Position	Residue	Chain
Hydrophobic	4	PHE	eL27	107	PHE	COX-2
	4	PHE	eL27	108	LEU	COX-2
	4	PHE	eL27	111	ALA	COX-2
	12	LEU	eL27	92	ILE	COX-2
	12	LEU	eL27	96	PHE	COX-2
	14	LEU	eL27	84	PRO	COX-2
	14	LEU	eL27	89	VAL	COX-2
	14	LEU	eL27	92	ILE	COX-2
	15	ALA	eL27	82	LEU	COX-2
	15	ALA	eL27	84	PRO	COX-2
	75	TYR	eL27	82	LEU	COX-2
	81	MET	eL27	100	TRP	COX-2
	81	MET	eL27	112	ILE	COX-2
	81	MET	eL27	92	ILE	COX-2
	81	MET	eL27	93	LEU	COX-2
	85	TYR	eL27	99	PHE	COX-2
	129	TRP	eL27	96	PHE	COX-2
	134	LEU	eL27	91	TYR	COX-2
	134	LEU	eL27	92	ILE	COX-2
	134	LEU	eL27	96	PHE	COX-2
	136	PHE	eL27	91	TYR	COX-2

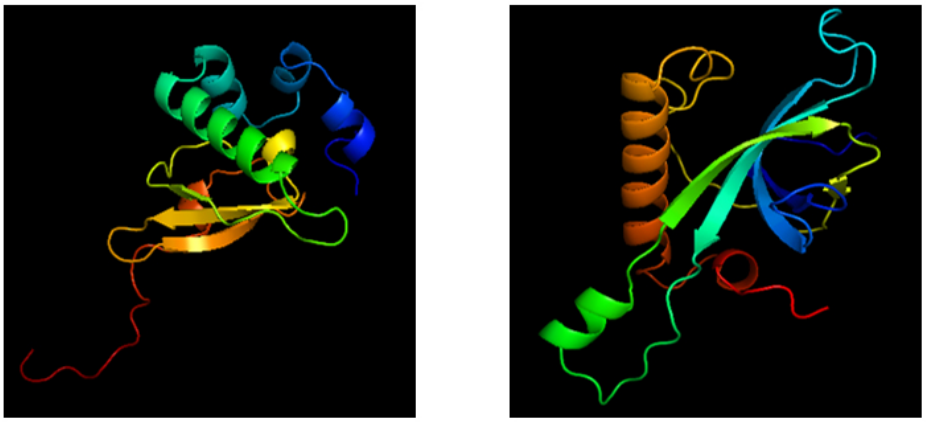

Figure 1: (a) uS19 protein model as viewed using PyMOL. (b) eL27 protein model as viewed using PyMOL.

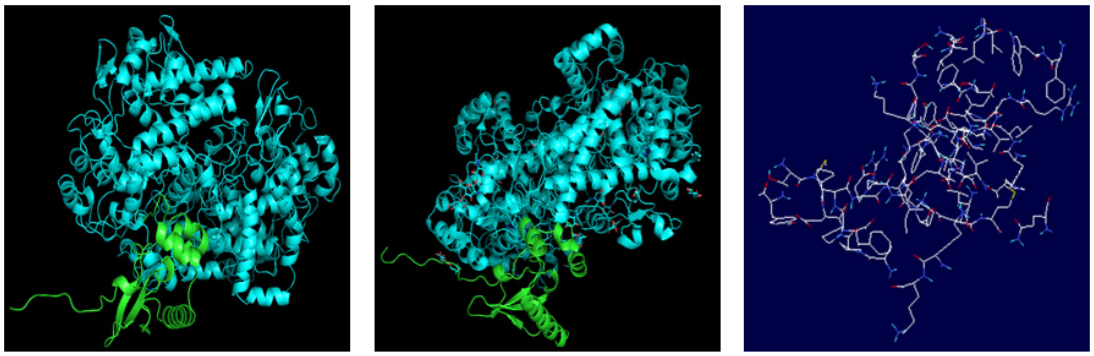

Figure 2: (a) uS19-COX-2 complex model from ClusPro as viewed using PyMOL. (b) uS19-COX-2 complex model from Patch-Dock. (c) Illustration of the interface residues (less than 5 Å) of the uS19-COX-2 complex viewed using Swiss PdbViewer.

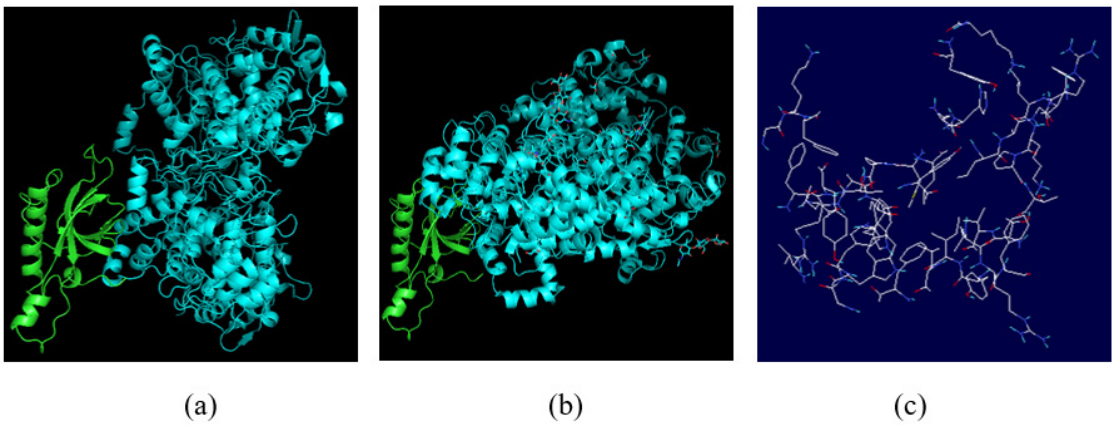

Figure 3: (a) eL27-COX-2 complex model from ClusPro as viewed using PyMOL. (b) eL27-COX-2 complex model from Patch-Dock. (c) Illustration of the interface residues (less than 5 Å) of the eL27-COX-2 complex viewed using Swiss PdbViewer.